Radiation Measurements 46 (2011) 473–476

Contents lists available at ScienceDirect

Radiation Measurements

journal homepage: www.elsevier.com/locate/radmeas

TL and OSL properties of $KAlSi_3O_8$:Mn, obtained by sol–gel process

Elcio Liberato Pires [a,*], Sonia Hatsue Tatumi [b], Juan Carlos Ramirez Mittani [b], Linda V.E. Caldas [c]

[a] Escola Politécnica da Universidade de São Paulo, Av. Prof. Luciano Gualberto, Travessa 380, 05508-900, São Paulo-SP, Brazil
[b] Faculdade de Tecnologia de São Paulo (FATEC-SP), Praça Cel. Fernando Prestes, 30, 01124-060, São Paulo-SP, Brazil
[c] Instituto de Pesquisas Energéticas e Nucleares (IPEN/CNEN), Comissão Nacional de Energia Nuclear, Av. Lineu Prestes, 2242, 05508-000, Cidade Universitária, São Paulo-SP, Brazil

ARTICLE INFO

Article history:
Received 16 November 2010
Received in revised form
14 February 2011
Accepted 15 February 2011

Keywords:
Thermoluminescence
Optically Stimulated Luminescence
Sol–gel
TLD-dosimetry
Luminescent glasses

ABSTRACT

Thermoluminescence (TL) and Optically Stimulated Luminescence (OSL) properties of $KAlSi_3O_8$:Mn glasses obtained through the sol–gel technique were investigated. Samples were obtained with five different molar concentrations of 0.25, 0.5, 1, 2 and 5 mol% of manganese. Transmission Electronic Microscopy (TEM) indicated the occurrence of nanoparticles composed by glass matrix elements with Mn. Best results for TL response were obtained with 0.5 mol% Mn doped sample, which exhibits a TL peak at 180 °C. The TL spectrum of this sample presents a broad emission band from 450 to 700 nm with a peak at 575 nm approximately. The emission band fits very well with the characteristic lines of the Mn^{2+} emission features. According to this fact, the band at 410 nm can be ascribed to $^6A_1(S) \rightarrow {}^4A_1(G)$, $^4E(G)$ transition, while the 545 nm band can be attributed to the superposition of the transitions $^6A_1(S) \rightarrow {}^4T_2(G)$ and $^6A_1(S) \rightarrow {}^4T_1(G)$. The dependence of the TL response with the energy of X-rays (27–41 keV) showed a small decrease of the TL intensity in the high energy region. Excitation with blue LEDs showed OSL in the UV region with a fast decay component.

1. Introduction

Aluminosilicate glasses doped with rare-earth elements and semi-metals are commonly produced for use as luminescent materials, in the manufacture of light emitting diodes and optical devices (Andrade et al., 2009; Pouxviel et al., 1989). However, there are no studies about the properties of dosimetric aluminosilicate glasses. Recently, Fuochi et al. (2009) cited some dosimetric properties of commercial window glasses irradiated with gamma-rays and electron-beams, showing that the silicate glasses are promising materials for ionizing radiation dosimetry. They concluded that this kind of material could be used as routine dosimeters within a certain dose range.

Thus, in this work an experimental study about the morphology and luminescent properties of $KAlSi_3O_8$:Mn glass, produced by sol–gel technique with different Mn concentrations, is presented. The sample morphology was investigated with TEM analyses and the effect of the Mn incorporation on the luminescent properties of the samples was studied through the Thermoluminescence (TL) and Optical Stimulated Luminescence (OSL) techniques.

The main dosimetric properties of $KAlSi_3O_8$:Mn glass, such as TL and OSL dose–response, fading, calibration curves and energetic dependence of the response are presented.

2. Materials and methods

The $KAlSi_3O_8$:Mn glasses were prepared with stoichiometric amounts of Aluminum sec-butoxide (ASB) (0.02 mol), tetraethyl-orthosilicate (TEOS) (0.06 mol), and KOH (0.02 mol). In order to perform the hydrolysis process, which induced the separation of the organic radical from the metal, 10 ml of distilled water was added to ASB and TEOS, and 20 ml of water was added in the KOH (Brinker and Scherer, 1990).

The reagents were stirred for 5 min at the temperature of 80 °C. Mn (0.25, 0.5, 1, 2 and 5 mol%) was introduced in the carbonates form, the concentration values were chosen analyzing the usual quantities found in the natural aluminosilicates (Bitencourt et al., 2006). The solution was again agitated for 20 minutes. As the medium is strongly basic, due to the addition of KOH, the carbonates are dissociated and incorporated into the material.

In general, to accelerate the hydrolysis process, in the majority of the synthesis by sol–gel which uses metal-alkoxide reagent, a small amount of a strong acid, such as HCl, is added. However, another mechanism of hydrolysis acceleration, found in the literature, takes into account the addition of one base. In this case, potassium was chosen because it is part of the final required composition. The obtained gel was stirred for 5 min, and then the heating was turned off. Afterwards, the gel was dried for 24 h at 70 °C. At this time any remaining water and substances derived

* Corresponding author. Tel.: +55 11 33222274; fax: +55 11 33222231.
E-mail address: elcioliberato@usp.br (E.L. Pires).

1350-4487/$ – see front matter © 2011 Elsevier Ltd. All rights reserved.
doi:10.1016/j.radmeas.2011.02.005

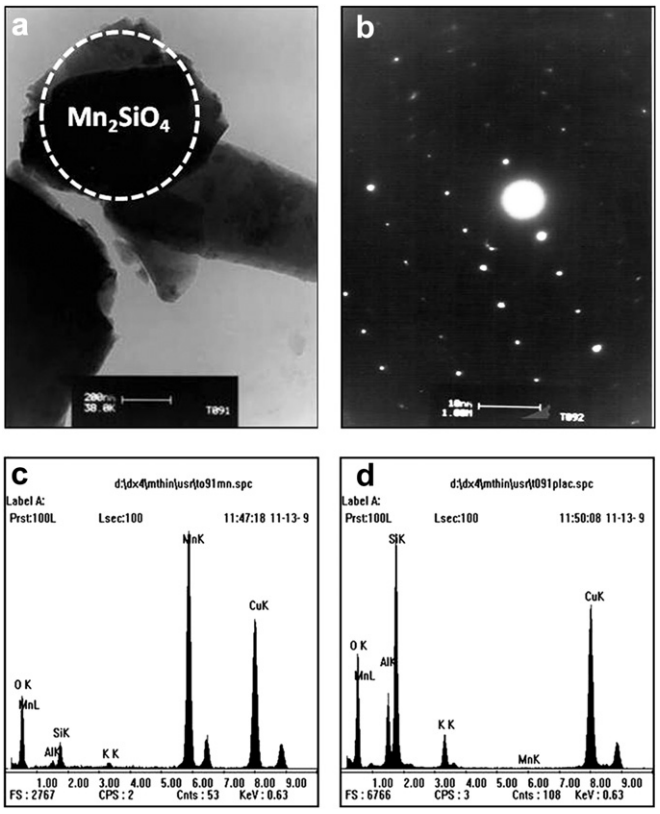

Fig. 1. a) TEM images of $KAlSi_3O_8$ glass doped with Mn showing a nanocrystals cluster inside the glass matrix; b) electron diffraction pattern of the nanoparticle; c) EDS results of the nanocrystals; d) EDS results of the glass matrix.

from the process were evaporated and the sample was obtained in the hydroxide composition.

Finally, $KAlSi_3O_8$:Mn glass was obtained by calcination of the hydroxide for 4 h at 1100 °C, with heating and cooling rates of 5 °C/min. It was experimentally verified that these parameters produced glasses with the best luminescence response.

The X-ray powder patterns of the samples were recorded using a diffractometer of the Rigaku Corporation; model MiniFlex II, which confirmed the amorphous state of the samples.

The morphological characteristics of the samples were analyzed using a Philips CM200 Transmission Electronic Microscope equipped with Energy Dispersive Spectrometer (EDS) operating at 160 keV. Some Cu contamination from the sample holder could be observed in all EDS results (Fig. 1c and d).

TL and OSL measurements were performed in an oxygen-free nitrogen atmosphere using a Daybreak Nuclear and Medical Systems Inc, model 1100-series TL/OSL reader, and the heating rate was 5 °C/s. TL measurements were taken in the UV (290–370 nm) and VIS (340–610 nm), using the optical filters Schott U-340 and BG-39, respectively.

TL spectra of the samples were obtained in a Varian 500 Cary Eclipse Fluorescence Spectrometer which was coupled to the TL/OSL reader by a waveguide.

OSL measurements were taken using an array of blue (470 nm) LEDs for sample excitation and detected in the UV with a Schott U-340 optical filter.

All gamma irradiations were performed at room temperature (RT) with a ^{60}Co source with the dose rate of 28.7 Gy/h. The irradiations with X-rays were carried out with a Rigaku Denki generator, model Geigerflex, with a Philips tube model PW/2184/00 (tungsten target and beryllium window, 60 kV); the dose was 1 Gy.

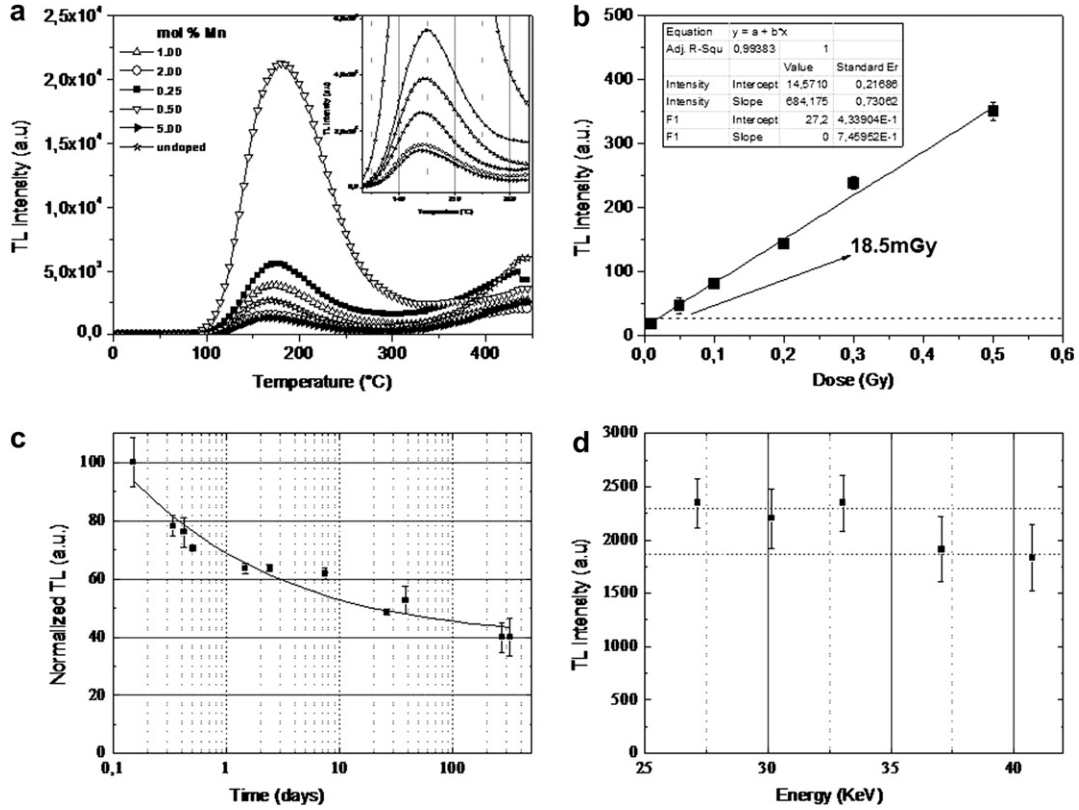

Fig. 2. a) TL glow curves obtained in the VIS of undoped and samples doped with different concentrations of Mn (0.25, 0.5, 1, 2 and 5 mol%); b) TL response versus γ-rays doses of $KAlSi_3O_8$ doped to 0.5 mol% Mn; c) fading experiment results performed at RT of the same cited sample; d) energetic dependence of the TL response.

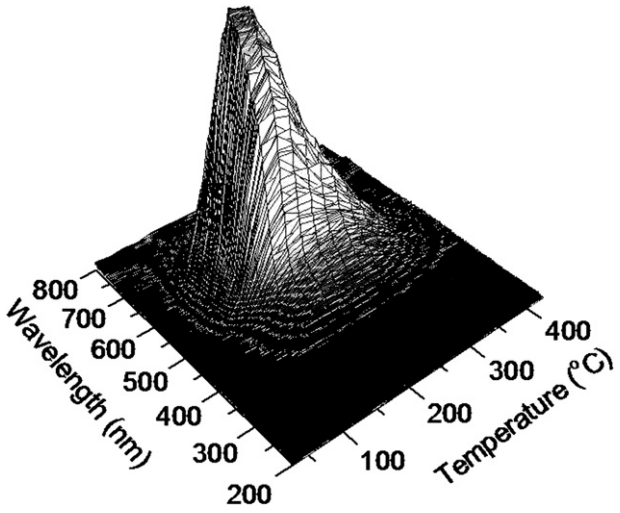

Fig. 3. TL spectrum of $KAlSi_3O_8$ doped to 0.5 mol% Mn.

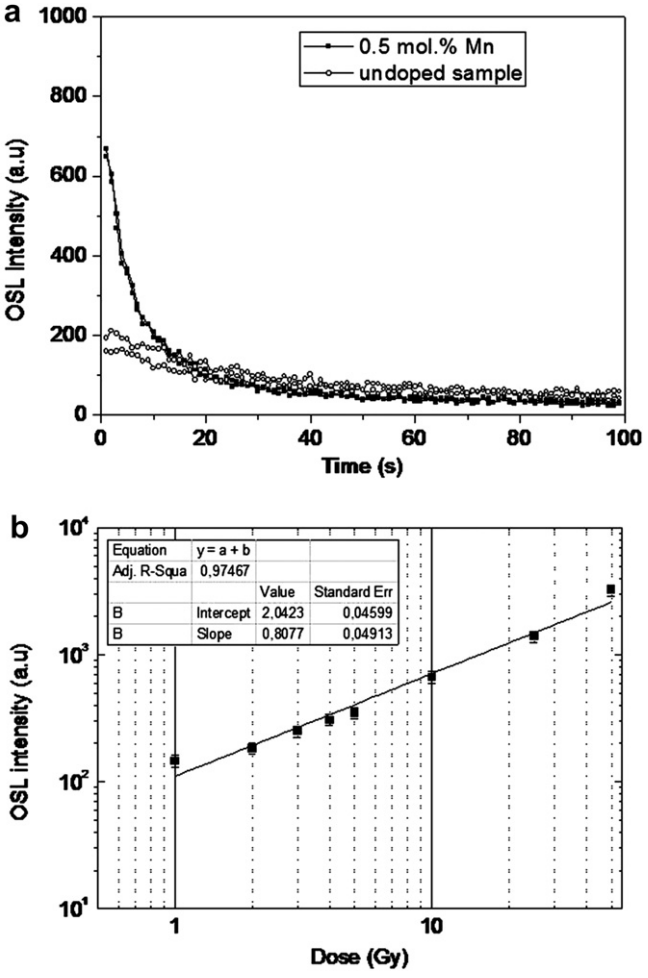

Fig. 4. a) OSL decay curves of the undoped $KAlSi_3O_8$ and doped to 0.5 mol% Mn, detected in the UV and excited at 470 nm and gamma-irradiated with a dose of 10 Gy; b) OSL response versus gamma-rays doses of $KAlSi_3O_8$ doped to 0.5 mol% Mn.

3. Results and discussion

TEM images and EDS results of $KAlSi_3O_8$:Mn showed a predominant vitreous structure (Fig. 1a) and nanoparticles with about 200 nm of size, which are composed by the same glass matrix elements with Mn (Fig. 1b).

Fig. 2a shows TL glow curves, obtained in the VIS, of undoped and samples doped with different concentrations of Mn. The undoped sample shows a glow curve with one broad TL peak at around 165 °C and another undefined one at high temperature, which did not show much reproducibility with the dose. The improvement of Mn doping was verified with the increase of the low temperature peak intensity. The maximum intensity was obtained with 0.5 mol% Mn doped sample, which was 4.6 times higher than those supplied by the undoped sample. The TL dose–response curve of this sample is shown in Fig. 2b. Using the 165 °C TL peak and gamma irradiations, the minimum detection dose was about 18.5 mGy, which verifies that the sample has a high TL emission. Fig. 2c shows the fading experiment results performed at RT monitored during 360 days. The decay rate was about 35.4% in the first 24 h, tending to a constant value after 10 days. The energy dependence of the TL response was analyzed within the 27–41 keV interval using X-rays, and a slow decay at high energy region (Fig. 2d) was observed.

In order to analyze the TL emission with more details, the TL spectrum of this sample was obtained and it is shown in Fig. 3. It presents a broad emission band from 450 to 700 nm with a peak at 575 nm approximately, and it fits very well with the characteristic lines of the Mn^{2+} emission features. According to this fact, the band at 410 nm can be ascribed to $^4A_{1g}(G)$, $^4E_g(G) \rightarrow {}^6A_{1g}(S)$ transition, while the 545 nm can be attributed to the transition $^4T_{1g}(G) \rightarrow {}^6A_{1g}(S)$ in an octahedral field.

A very low OSL intensity supplied with the undoped one was observed (Fig. 4a), comparing to other Mn doped samples. A high intensity signal with a fast OSL decay signal was obtained with Mn doped sample and it is about 10 times higher than OSL signals supplied with undoped one. The decay can be fitted by a second order exponential decay equation, $I = A_1\exp(-x/\tau_1) + A_2\exp(-x/\tau_2)$, $A_1 = (250 \pm 4)$, $\tau_1 = (5.2 \pm 0.1)$, $A_2 = (58.4 \pm 2.1)$ and $\tau_2 = (48.2 \pm 1.8)$ (McKeever and Chen, 1997). A linear dose–response of the OSL for samples irradiated with gamma-rays (Fig. 4b) was verified.

4. Conclusions

The results show that this matrix favored the Mn^{2+} center creations, and the TL emission mechanism can be explained as due to the recombination of Mn^{3+} center with an electron in the heating process, when the TL process is carried out. Then, the Mn^{2+*} in excited state is created and TL is emitted subsequently due to Mn^{2+*} relaxation into fundamental state; the Mn^{3+} is produced previously by exposure to ionizing radiation; this assumption was consistent with Dotzler et al. (2007) work. The sample with 0.5 mol % of Mn supplied the highest luminescence intensity. In the samples with the lowest TL response; the Mn ions, probably, have different valence numbers; another possible cause is the concentration quenching phenomenon. This phenomenon may be attributed to the migration of the excitation energy between Mn^{2+} ions pairs; the excitation energy is transferred from one Mn^{2+} to its adjacent Mn^{2+} by a non-radioactive transition, to a quenching defect state (Khosravi et al., 1995; Murugadoss et al., 2010). In the present case the samples show Mn_2SiO_4 nanoparticles occurrence, which are agglomerated forming clusters in some regions of the glass leading to an inter-ion interaction.

The anti-Stokes emission was observed in the OSL measurements, where the UV emission was produced under blue excitation. The OSL response was proportional to gamma dose. Similar results

about anti-Stokes OSL emission in the ultraviolet region, of Mn doped sample, has not been reported in the literature yet, only phosphors presenting Stokes emission, as in Henke et al. (2007) and Dotzler et al. (2007) papers.

The results related to dosimetric properties indicate that $KAlSi_3O_8$:Mn glass present possibility of use as luminescence dosimeters.

References

Andrade, L.H.C., Lima, S.M., Novatski, A., Steimacher, A., Rohling, J.H., Medina, A.N., Bento, A.C., Baesso, M.L., Guyot, Y., Boulon, G., 2009. A step forward toward smart white lighting: combination of glass phosphor and light emitting diodes. Appl. Phys. Lett. 95, 081–104.

Bitencourt, J.F., Kinoshita, A., Munita, C.S., Tatumi, S.H., 2006. Luminescence and ESR properties of Brazilian feldspar. Radiat. Meas. 41, 948–953.

Brinker, C.J., Scherer, G.W., 1990. Sol–Gel Science: The Physics and Chemistry of Sol–Gel Processing. Academic Press Inc., San Diego.

Dotzler, C.J., Williams, G.V.M., Edgar, A., 2007. Thermoluminescence, photoluminescence and optically stimulated luminescence properties of X-ray irradiated $RbMgF_3:Mn^{2+}$. Phys. Status Solidi C 4 (3), 992–995.

Fuochi, P., Corda, U., Lavalle, M., Kovács, A., Baranyai, M., Mejri, A., Farah, K., 2009. Dosimetric properties of gamma and electron-irradiated commercial window glasses. Nukleonika 54 (1), 39–43.

Henke, B., Rogulis, U., Schweizer, S., 2007. Optical and electron paramagnetic resonance studies on radiation defects in Mn-activated $RbCdF_3$. Phys. Status Solidi C 4 (3), 1071–1074.

Khosravi, A.A., Kundu, M., Kuruvilla, B.A., Shekhawat, G.S., Gupta, R.P., Sharma, A.K., Vyas, P.D., Kulkarni, S.K., 1995. Manganese doped zinc sulphide nanoparticles by aqueous method. Appl. Phys. Lett. 67, 2506–2508.

McKeever, S.W.S., Chen, R., 1997. Luminescence models. Radiat. Meas. 27 (5/6), 625–661.

Murugadoss, G., Rajamannan, B., Ramasamy, V., 2010. Synthesis, characterization and optical properties of water-soluble $ZnS:Mn^{2+}$ nanoparticles. J. Lumin. 130, 2032–2039.

Pouxviel, J.C., Dunn, B., Zinkt, J.I., 1989. Fluorescence study of aluminosilicate sols and gels doped with hydroxy trisulfonated pyrene. J. Phys. Chem. 93, 2134–2139.